JMEPEG (2010) 19:1015–1021
DOI: 10.1007/s11665-009-9581-9

1059-9495/$19.00

Characteristics of Diffusion Annealing Between Martensitic Stainless Steel and Nickel in the Form of Coating and Foil

A. Araee and H. Sabetghadam

(Submitted July 16, 2009; in revised form September 29, 2009)

Characteristics of interaction between martensitic stainless steel type AISI 410 with nickel in the form of coating layer and foil were investigated. Nickel was coated on AISI 410 substrate by electroplating in various thicknesses (6-16 μm). The 300-μm-nickel with purity of 99.9% was employed as a foil layer. All specimens were annealed in the temperature range of 700-900 °C for 5, 10, 15, and 60 min. Optical microscopy, SEM and EPMA analyzer were carried out in order to characterize the interdiffusion behavior differences between nickel and AISI 410 while using nickel layer in different form. It was observed that the thickness of nickel coating had a minor effect during annealing on the interaction between Ni and substrate at faying surface. However, the results show that the interaction of nickel coating layer with base material is much faster than foil layer during annealing process. This study suggests that the coating layer diffused faster to the substrate than foil layer; moreover, in the former case, heavy outer load was omitted. The concentration profiles were plotted for two cases. Although in case of using layer in the form of coating the annealing time was relatively short (5-15 min), it was observed that the concentration profiles for main elements had shapes close to the theoretical curve. For various thicknesses (6-16 μm) of Ni coating, the experimental results show that the interaction at faying surface caused the thickness of nickel coating growth. The diffusion zone width was plotted against the annealing temperature and time for both cases and the growth of the diffusion zones was compared.

Keywords diffusion bonding, interdiffusion, martensitic stainless steel, surface roughness

1. Introduction

Martensitic stainless steels (MSS) have been used in components operating under wear and corrosion resistance. These types of steels show high mechanical properties and also have the capacity to achieve high hardness during heat treatment (Ref 1, 2). These steels are widely used in industrial applications such as tools holder's, plastic dies, and medical devices (Ref 3). However, one of another application of MSS was found in aerospace for manufacturing the housing of bearings in jet engines. These types of stainless steels have sufficient percentage of chromium, generally, more than 11% but the percentage of nickel in them is very low. The interaction between nickel and MSS at elevated temperatures is important due to the application of this combination in diffusion bonding process for joining MSS with other metals. On the other hand, by coating the nickel on the surface of MSS and applying the suitable heat-treatment process, it is possible to enhance the corrosion resistance and stress resistance. Because after nickel diffused, a thin layer of austenitic enrichment of nickel and chromium was formed on the surface of MSS (Ref 4). It is well known that nickel is the most used interlayer for many different materials which are subjected to diffusion bonding. The use of appropriate intermediate materials can minimize the formation of the brittle intermetallics, which in turn further increases the mechanical properties of the diffusion-bonded joints. Nickel has substantial solid solubility in iron and Kamat et al. reported that a nickel-stainless steel diffusion couple is free from intermetallics (Ref 5). The binary phase diagram of Fe-Ni shows that compound of Fe-Ni is formed for 74-84 at.% Ni at ~500 °C and due to the existence of Cr to the substrate, Ni-Cr forms an ordered compound of at 22-32 at.% Cr at ~600 °C (Ref 6, 7). The interdiffusion behaviors between pure metals and alloys, in which concentration gradients of the components are present, have been investigated by many authors (Ref 8, 9). However, there are still many metals and alloys for which much less information related to interdiffusion characters can be found in the literature.

The goals of the present study were to investigate the interaction behaviors of nickel (in two forms of foil and electroplated) with MSS type AISI 410 through the diffusion annealing process. Additionally, comparing the diffusion zones in two cases of using nickel coating and foil layer after annealing have been considered in this study. The growth of nickel coating during annealing process for all samples was measured. These measurements are interesting due to the thickness of the nickel layer after annealing is important for diffusion bonding process. In this work, the Krikendall effect

A. Araee, School of Mechanical Engineering, University of Tehran, Tehran, Iran; and **H. Sabetghadam**, School of Metallurgy and Material Engineering, University of Tehran, Tehran, Iran. Contact e-mail: h.sabetghadam@gmail.com.

was observed at faying surfaces in both cases and was explained by the difference in diffusivities of the diffusion species.

2. Experimental Procedure

The commercial martensitic stainless steel grade AISI 410 was used in the form of plate with thickness of 2 mm. The chemical composition of this alloy is shown in Table 1. It is noticeable that the microstructure of as-cast and wrought forms of this material is different. Preliminary attempts were made by recent authors to evaluate the effect of different thickness of nickel coating on interdiffusion between Ni/AISI 410 couple. Three rectangular pieces (as wrought) with sizes of 20×20 cm^2 were used and Ni was coated on them in thickness of 6, 10, and 16 μm by electroplating process, respectively. The surface roughness of specimens before and after the coating process was measured by profilometer (Turbo Roughness V3.34). To characterize the effect of heat-treatment parameters on diffusion Ni/AISI 410 couple, from each thickness of Ni coating (6, 10, and 16 μm) 15 samples were cut in the form of coupons having dimensions of $10 \times 15 \times 2$ mm^3 in size. For all specimens, the process of coating nickel on the base metal was carried out in a Watt's nickel bath consisting of 330 g/L of nickel sulfate, 45 g/L nickel chloride, and 45 g/L boric acid. The bath temperature, PH, and current density were hold in 60 °C, 5 and 10 A/dm^2, respectively. Before coating, a number of pre-treatment procedures were applied to produce a highly clean surface; other procedures necessary for preparing stainless steel for electroplating are done that are fully described in ASTM B254. The heat treatment on nickel-coated specimens was carried out in a 10^{-5} Torr-vacuum furnace with heating rate of 30 °C/min and at the temperature range of 700-900 °C at 5, 10, and 15 min Table 2 shows the details of annealing trials. For samples with nickel foil, the same condition was used but the holding time was 60 min. Also, the extra uniaxialy 12 MPa pressure was applied along the longitudinal direction of these samples. This heavy pressure was introduced by hot vacuum press and caused to overcome the corrugation surfaces and to help the increase of real contact between surfaces and diffusivity of species. All the samples were cooled in a furnace with cooling rate of 20 °C/min. The annealed samples were sectioned perpendicular to the faying surface and processed by conventional metallographic techniques for further studies. The microstructure of the couples was studied using an optical microscopy and SEM (Jeol 50X) equipped with EDS. The concentration profiles across the interface were established by an electron probe micro-analyzer (EPMA, LEO-ZIESS) equipped with three wavelength dispersive spectrometers. The operating voltage and stabilized beam current were kept at 20 kV and 20 mA, respectively. LiF crystal was used to diffract FeK_α, CrK_α, and NiK_α. The variation in the hardness in an area sufficiently close to the interface was measured by the microhardness tester (LEITZ WETZLAR 8375) at different points with a diamond micro-indenter using a 100 g loading pressure with a 15 s dwelling time.

Table 1 Chemical composition of 410 stainless steel (wt.%)

Element, wt.%								
Fe	**C**	**Si**	**Mn**	**P**	**S**	**Cr**	**Ni**	**Cu**
Bal.	0.14	0.30	0.20	0.02	0.01	12.70	0.20	0.10

Table 2 Diffusion zone and thickness of nickel after annealing with initial thickness of 16 μm

Samples	Temperature, °C	Time, min	Diffusion zone, μm	Final thickness, μm
C11	700	5	…	16.0
C12	750	5	3.9	15.5
C13	800	5	1.5	18.5
C14	850	5	2.0	17.2
C15	900	5	2.5	18.0
C21	700	10	2.1	15.6
C22	750	10	4.5	16.1
C23	800	10	2.0	18.1
C24	850	10	5.0	16.4
C25	900	10	4.0	20.0
C31	700	15	…	16.0
C32	750	15	4.3	15.0
C33	800	15	2.2	15.7
C34	850	15	4.5	19.4
C35	900	15	3.5	18.0

3. Results and Discussion

3.1 Surface Contact

Experiments have shown that the roughness of contact surfaces has a significant impact on the bonding process (Ref 10). Some theoretical analyses have been carried out to investigate this issue (Ref 11, 12). There are numerous statistical parameters that may be calculated from the profilometry data. The most common parameters calculated from the roughness profiles are R_a, R_z, and R_{ku}, which refer to arithmetical mean deviation, the average of ten point height, and the peak height distribution, respectively. Figures 1 and 2 show the P-profile (height density curve) and the W-profile (waviness curve) of AISI 410 surface, before and after being coated with nickel, respectively. In Fig. 1, the surface of MSS was grinded with #600 emery paper and Fig. 2 shows the morphology of surface after 15-μm-nickel coating on the base metal. The root mean roughness of prepared surfaces by #600, emery paper and surface after nickel coating were obtained as 0.16 and 0.19 μm, respectively The W-profile curve shows the mean of high and depth of peaks and valleys and their deviation from straight line, (described in M1 DIN 4777) while the P-profile shows the distribution of peaks along the straight line. As can be expected, after coating the nickel on the surface of MSS, the roughness of coating surface increase compared with the roughness of the substrate. However, in this investigation, the surface roughness before nickel coating has a crucial role in mutual diffusion during annealing.

Chen et al. have surveyed the effect of surface roughness on diffusion bonding between Al and Cu under uniaxialy pressure. In this point, the diffusion bonding process was divided into three stages. In the first stage, the rough surface deforms under stress before heating, causing the contact area to increase. In the

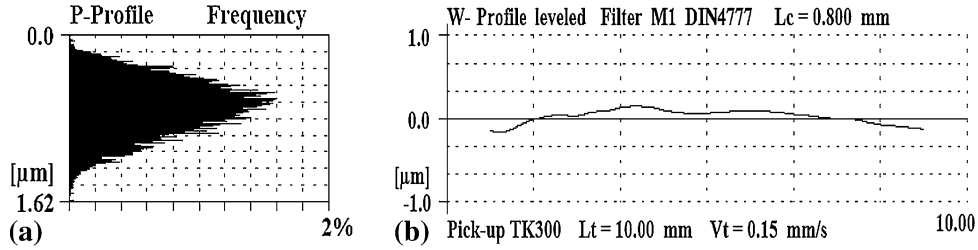

Fig. 1 The 2D profilometery of AISI 410 surface roughness prepared by #600 emery paper before coating nickel: (a) P-profile and (b) W-profile (R_a = 0.16 µm)

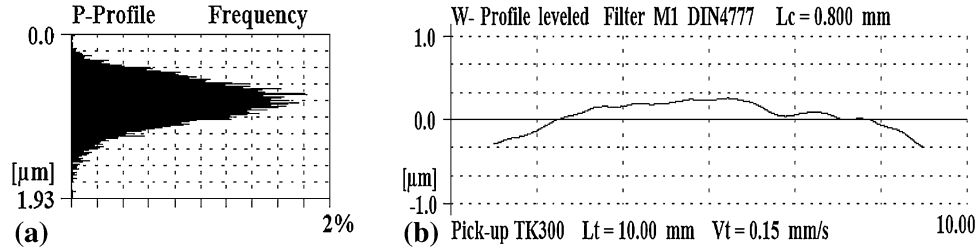

Fig. 2 The 2D profilometery of AISI 410 surface roughness after coating nickel: (a) P-profile and (b) W-profile (R_a = 0.19 µm), the roughness increased compared with case of before coating

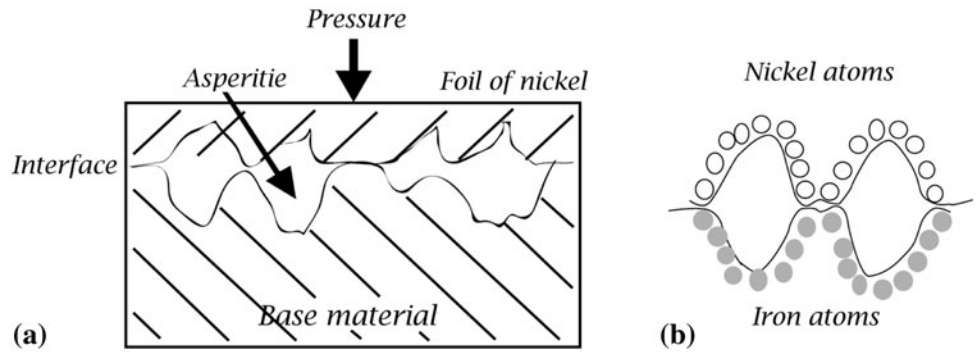

Fig. 3 Using a foil interlayer for diffusion bonding: (a) plastic deformation occurs but still asperities exist; (b) whole atoms cannot diffuse to each side

second stage, the softer surface undergoes significant deformation as temperature increases, causing the interstices to disappear and leading to fully intimate contact of the surfaces. The last stage is the diffusion of atoms at constant temperature (Ref 10). This scheme is consistent with Derby's theoretical model (Ref 11, 13), which identified the possible diffusion bonding mechanisms as (i) plastic deformation of surface asperities; (ii) power-law creep deformation of the surface; (iii) diffusion of matter from interfacial void surfaces to growing necks; and (iv) diffusion of matter from bonded regions on the interface to growing necks.

It should be noted that the diffusion of nickel coating to the base metal during annealing is somewhat different from when using nickel in the form of foil. In the case of Ni coating due to the nature of electroplating process, no asperities exist between the two surfaces and atom types are in contact with each other. The occurrence of full contact between two surfaces eliminates heavy outer pressure. Whereas in the case of using nickel layer as a foil, the ridge-to-ridge contact caused only a small part of the surfaces are brought in contact (Ref 14). In the latter case, despite plastic micro-deformation occurring under pressure at elevated temperatures and causing most of the asperities to vanish, however, some voids still remain and prevent the whole surfaces from coming into contact. The lack of full contact between the two surfaces makes it time-consuming to achieve atoms diffusive to each side. Figure 3 shows the schematic of real contact between surfaces of Ni foil and substrate. In this case, only a part of whole atoms can diffuse to the other sides. Figure 4 shows the backscatter images of the interface of the sample with Ni coating treated at 800 °C for 10 min, where no gaps are visible at high magnification. Figure 5 shows the optical micrograph and backscatter image of the microstructure of Ni-coating/MSS couple which were treated at 850 °C for 15 min. By increasing temperature and time, the micro-voids are dramatically reduced and also no gaps are visible at the interface. Figure 4(b) shows the sample with Ni foil which was treated at 800 °C for 60 min and 12 MPa, where the gaps are visible at lower magnification. The existence of gaps at the

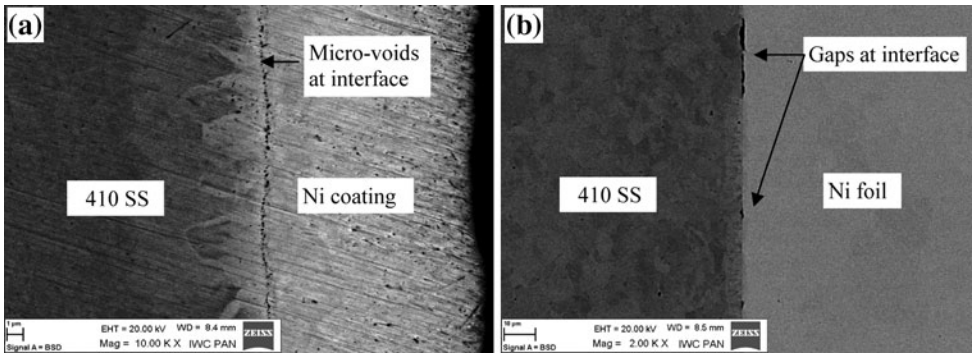

Fig. 4 Backscatter images of interfaces: (a) sample with Ni coating treated at 800 °C for 10 min, no gaps are visible at high magnification (10,000×); (b) sample with Ni foil treated at 800 °C for 60 min and 12 MPa, the gaps are visible at lower magnification (2000×)

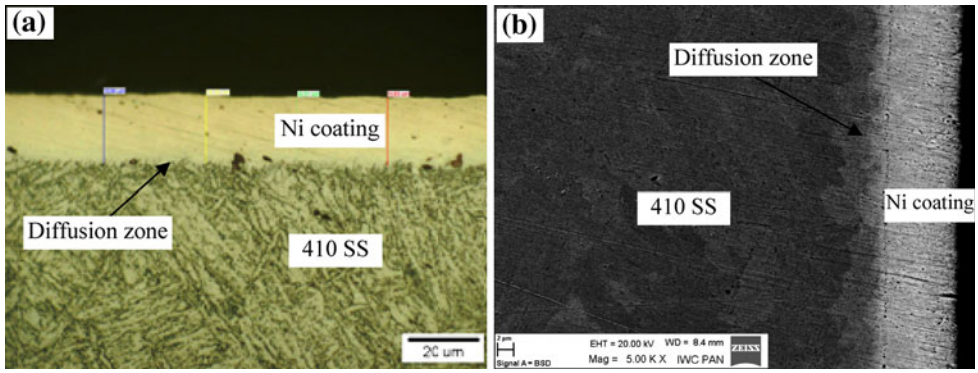

Fig. 5 (a) Optical micrograph and (b) backscatter image showing the microstructure of Ni-coating/MSS couple treated at 850 °C for 15 min, no gaps are visible at the interface

faying surface caused the reduction of bond strength dramatically. Comparing the images in Fig. 4 shows that diffusion couples with Ni coating at the same temperature and shorter time is achieved than Ni foil. Whereas in the case of using Ni foil and at the longer time, by applying the pressure, many gaps are visible obviously at the faying surface.

Earlier, Kundu and Chatterjee (Ref 8) studied the interdiffusion behavior between a grade of titanium alloy and austenitic stainless steel and deduced that in the lower processing temperatures bond strength is minimal due to the lack of contact between the mating surfaces, even though the yield stress of the material still remains high. They reported that low processing temperature also leads to a minimum thermal excitation and limiting the extent of diffused alloying elements at diffusion interfaces.

In the case of coating layer, theoretically no gaps exist to prevent full contact between coating layer and base metal and atoms can migrate to other side easily. It can be deduced that, during annealing process by using Ni coating as an interlayer, the diffusion of atoms to the base material is much easier than in the form of foil layer. Although the roughness of surface has a considerable effect on interdiffusion in both cases, however, in case of Ni coating on substrate the surface roughness has significant effect on interdiffusion comparing to case of using the layer in the form of foil. It is clear that the smoother surface provides a greater contact area which increases the atomic diffusion paths during annealing and causes mutual diffusion to occur better than on rough surfaces.

Annealing process was conducted on specimens with Ni coating at 850 °C for 10 min and with Ni foil at 900 °C for 60 min under 12 MPa. For both cases, the electron backscattered images and concentration profiles (wt.%) of the major elements, i.e., Fe, Ni, and Cr, obtained from EPMA analyses across the diffusion interfaces are presented in Fig. 6 and 7, respectively. The concentration of all the elements was seen to vary smoothly within the diffusion zone. However, by comparing the concentration profiles between two cases, it revealed that the interdiffusion in the case of Ni coating occurs better than Ni foil. The concentration profile of nickel and iron across the interface in both cases clearly shows that the diffusion coefficient of the iron is greater than the nickel. It is also evident from the profiles that Fe penetrates deeper into the Ni side than Ni diffuses into MSS side. This difference may be attributed to the difference in the liquidus temperature of the two materials. As the melting point of pure Ni (1453 °C) is lower than the melting point of MSS (~1500 °C), Fe element tends to diffuse faster and deeper into the nickel side. The absence of intermetallic compounds in the diffusion zone at operation temperature (700-900 °C) is consistent with the ternary phase diagram of iron-nickel-chromium, with a large solid solution above 600 °C, as reported in the literature (Ref 9-15). Up to the 850 °C joining temperature, the diffusion zone is observed to be free from reaction products. The presence of Fe and Cr in the nickel side indicates substantial interdiffusion of the two alloying elements at bonding temperatures up to 850 °C. Similarly, Ni also migrates to the stainless

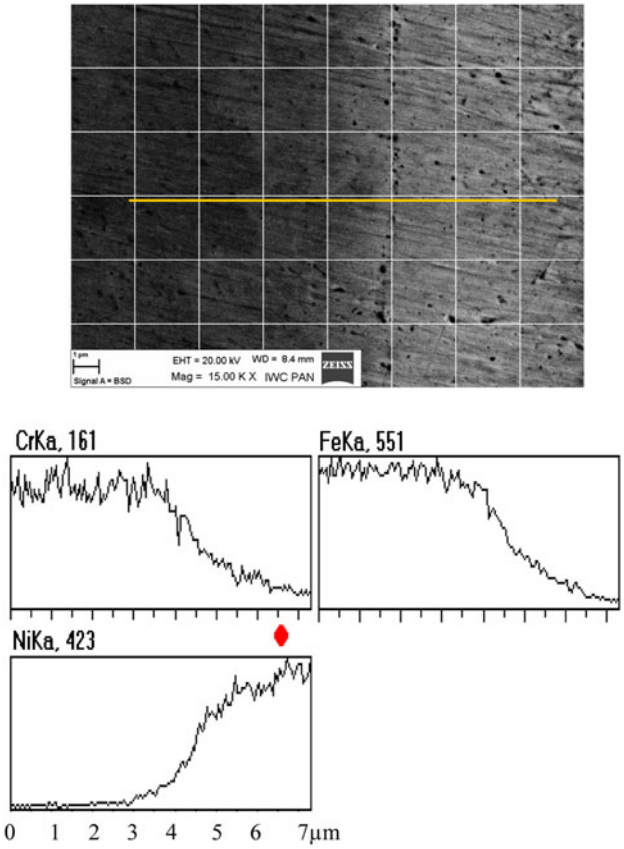

Fig. 6 Backscatter image and concentration profiles (5 wt.%) for the main elements treated at 850 °C for 10 min (Ni coating)

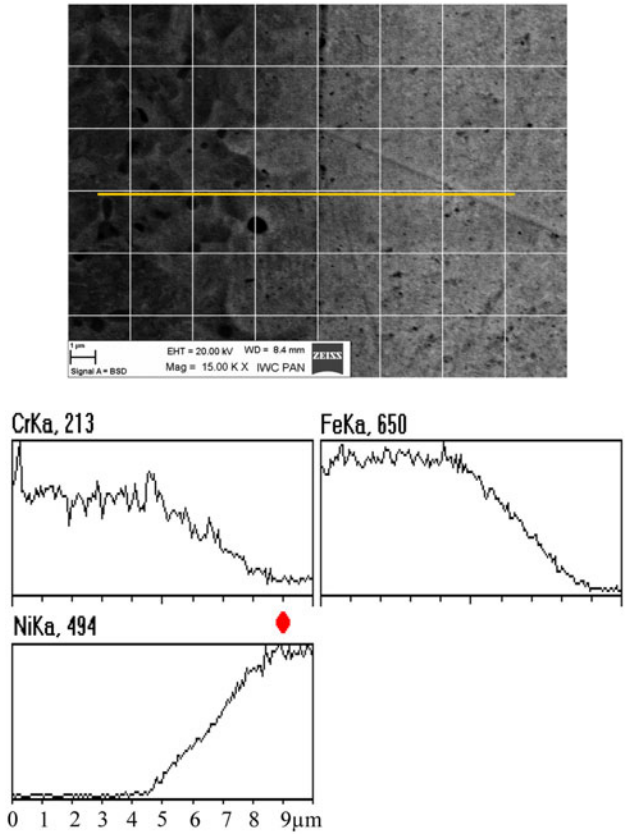

Fig. 7 Backscatter image and concentration profiles (wt.%) for the main elements treated at 900 °C for 60 min and 12 MPa (Ni foil)

steel substrate in significant quantity (~27.4-40.3 at.%) at the same temperature range.

3.2 Interdiffusion

Figure 8 shows the results of the growth of the Ni coating layer in different thickness (6, 10, and 16 µm) after interaction with AISI 410 substrate. The specimens were treated in the temperature range of 700-900 °C for 15 min. During the annealing process, interdiffusion occurs and causes the microstructure at faying surface to divide into three zones: base metal zone, diffusion zone, and the coating layer zone. Comparing the thickness of the layer before and after annealing in all cases shows an increase in the thickness of nickel coating. No significant effects were observed on the bond region due to the difference of thickness of Ni coating layer. The main reason for the growth of the nickel layer is that the initial pure nickel had changed during annealing to a Ni/Fe/Cr mixture, due to the outward diffusion of Fe and Cr. The existence of a high concentration of nickel at the interface caused the nickel atoms diffuse to the base metal during annealing, while from the base metal, iron and chromium atoms diffuse to the nickel layer. In other words, the flow rate of total atoms of Fe and Cr toward nickel layer is greater than that of nickel atoms to the base metal. Therefore, one can expect the thickness of the nickel layer to grow. To confirm the growth of the nickel coating thickness during annealing, EDS analyses were applied. The analyses revealed that the sum of iron and chromium percentages (7.9 + 8.6 = 16.5 wt.%) which diffused to the Ni coating layer is greater than the sum of nickel percentage

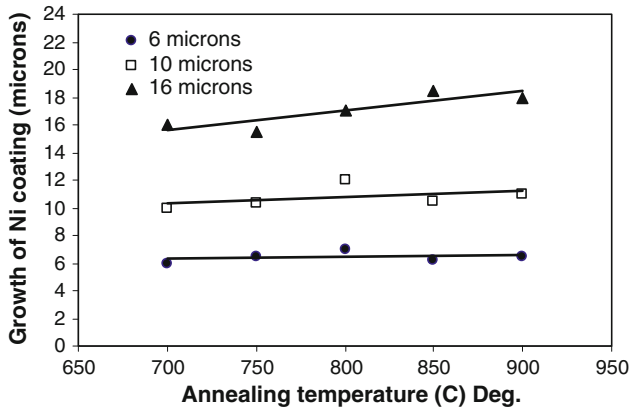

Fig. 8 Growth of Ni coating after annealing in temperature range of 700-900 °C for 15 min. Initial thickness of Ni was 6, 10, and 16 µm

(14.2 + 0.2 = 14.4 wt.%) diffused to the diffusion zone and base metal (see Table 3). The output of the EDS analyzer is shown in Table 3.

During annealing between Ni and AISI 410, it is assumed that the concentration gradient occurs along the X direction and it is governed by Fick's equation. In real alloy systems, the interdiffusion coefficient (D) of elements vary with concentration (Ref 16); however, no reports were found in the literature about interdiffusion coefficient of nickel to MSS. Kale et al. (Ref 16) reported the interdiffusion coefficient for Ni in Ni-Fe-Cr

Table 3 Results of EDS analyses of nickel diffusion coating on surface for sample treated at 850 °C for 10 min

	Elements, wt.%		
	Ni	Cr	Fe
Coating layer	83.2	8.6	7.9
Diffusion zone	14.2	12.2	71.8
Base metal	0.2	12.6	86.5

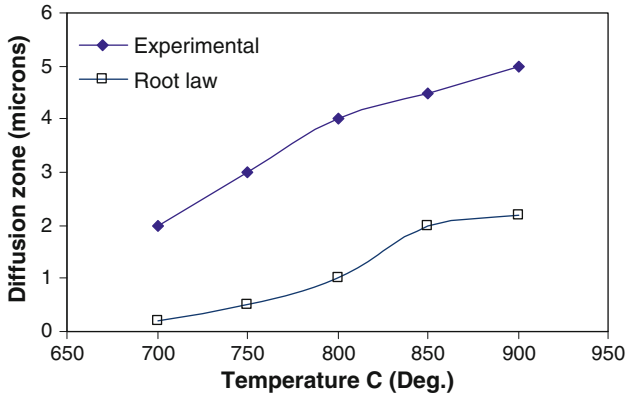

Fig. 9 Diffusion zone growth of Ni coating/MSS and comparison of the results from Eq 1 and experimental work, samples treated at 700-900 °C for 15 min

system at 1000 °C. As mentioned earlier, the mechanism of interdiffusion was different when nickel coating or foil layer was used. However, various studies have been recently done on interdiffusion coefficient between nickel layer (in the form of foil) and different types of stainless steels (Ref 16, 17). Yet, it is difficult to find match data on the interdiffusion coefficient between coating nickel and AISI 410. Interdiffusion coefficient between nickel coating and the MSS can also be estimated by applying the Boltzmann-Matano equation. A better solution to the problem of finding interdiffusion coefficient for ternary phase diagram or higher was suggested by Dayananda and Sohn (Ref 17).

3.3 Calculation of Diffusion Zone

For estimating the growth of diffusion zone, the general equation as follows can be used (Ref 16):

$$w = k\sqrt{t} \qquad \text{(Eq 1)}$$

where w is the width of the diffusion zone, t is the annealing time, and k is a constant defined by the Arrhenius relation:

$$k = k_0 \exp(-Q_k/RT) \qquad \text{(Eq 2)}$$

For calculating k in different annealing temperatures, k_0 and Q_k were adopted from the work of Laik et al. (Ref 18) as $k_0 = 2.7 \times 10^{-2}$ m s$^{-1/2}$ and $Q_k = 122.6$ kJ mol^{-1}, respectively.

In order to determine the thickness of diffusion zone for various annealing temperatures and times, Eq 1 and 2 were applied. The results from these equations and those from the experimental work for the case of Ni coating are plotted in Fig. 9. It can be seen that there is a large gap between the

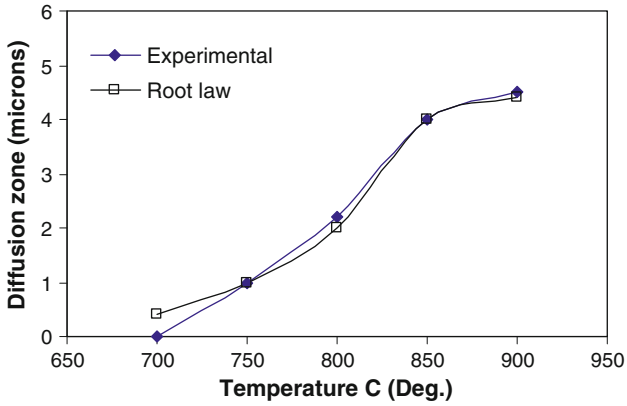

Fig. 10 Diffusion zone growth of Ni foil/MSS and comparison of the results from Eq 1 and experimental work, samples treated at 700-900 °C for 60 min and 12 MPa

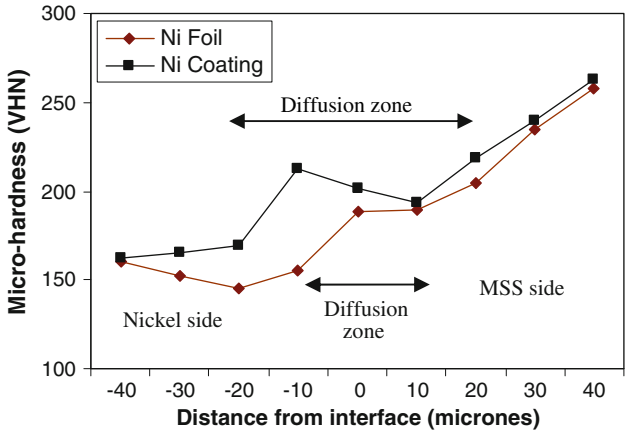

Fig. 11 Variation in the hardness across the diffusion zone of the Ni/MSS couples annealed at 850 °C for 15 min for Ni coating and 60 min under 12 MPa pressure for Ni foil

results of Eq 1 and the experimental work. It reveals that this equation is only valid for estimation of the growth of reaction zone when the interlayer is in foil form and consequently the annealing time would be quite long. Calculation of the diffusion zone in case of using coated layer needs another model. The growth of diffusion zone plotted from the results of experimental work and calculations according to Eq 1 for the case of nickel foil is shown in Fig. 10. In this case, better agreement was observed between experimental and Eq 1. It is clear that the growth of diffusion zone is directly related to an increase time and temperature of testing.

3.4 Micro-Hardness Behavior

The variation in the hardness across the diffusion zone for both cases was measured using a micro-hardness tester; the results are shown in Fig. 11. The profiles are obtained for heat treatment at temperature 850 °C for 15 min for Ni coating and 60 min under 12 MPa pressure for Ni foil. The hardness for both cases varied across the diffusion zone.

The more volume of interdiffused atoms in the case of Ni coating leads to phase constitution at the interface. The binary phase diagram of Fe-Ni system shows the presence of many

phases and solid solutions. But in this case and according to the XRD results (not given), the (γFe, Ni) solid solution and $FeNi_3$ phase were produced at diffusion zones in the sample treated at 850 °C for 15 min. The existence of this phase transition leads to changes in micro-hardness curves. In this manner, the existence of $FeNi_3$ and (γFe, Ni) phases caused the maximum and minimum points in the micro-hardness curves in the Ni coating case, respectively (see Fig. 11). In the case of using the Ni foil, because of the minor volume of interdiffused atoms, the width of diffusion zone is lower and the micro-hardness curve varied smoothly from the Ni side to the MSS side (as seen in Fig. 11).

4. Conclusions

The microstructure of the parent materials AISI 410 shows an acicular martensitic structure and dose not change during the annealing process. The AISI 410/Ni coating diffusion couples, bonded at 850 °C for 15 min, show excellent bonding without any gaps along the interface. Whereas in the AISI 410/Ni foil diffusion couples, bonded at 900 °C for 60 min and 12 MPa pressure, some gaps are visible along the interface. However, both the Ni coating and Ni foil exhibit good interaction with base metal and concentration profiles varying smoothly across the diffusion zone. This study suggests that the mechanism of interaction between base material and coating layer during the annealing process is quite different from when using layer in the form of foil. Nickel has higher values for diffusion coefficient than other components; however, the sum of flux of these components toward the nickel layer caused nickel coating growth. Increasing the annealing temperature would increase the interaction between Ni-Fe-Cr at the faying surface. At the lowest annealing temperature (700 °C), no interaction could be detected, whereas no significant effect was seen on the diffusion zone by increasing the annealing time. The increase in the thickness of the coated layer after annealing can be attributed to the fact that the sum of iron and chromium atoms migrated to the nickel layer is greater than nickel atoms that diffuse to the base metal. The values of penetration depth determined from roots law and experimental work for the both cases. The results show good agreement for the Ni foil and mismatch for coating layer.

References

1. P.T. Lovejoy, *Handbook of Stainless Steels*, Chap. 6, McGraw-Hill, New York, 1977, p 800
2. P. Unterweiser, H.E. Boyer, and J.J. Cubbos, *Heat Treatment Guide Standard and Practice Procedures for Steel*, ASM International, Materials Park, OH, 1983, p 257
3. D.H. Mesa, A. Toro, A. Sinatora, and A.P. Tschiptschin, The Effect of Testing Temperature on Corrosion–Erosion Resistance of Martensitic Stainless Steels, *Wear*, 2003, **255**, p 139–145
4. Z. Abdel Hamid, M.A. Abbas, and N. Gomaa, Enhancement of the Properties of Austenitic Stainless Steel by Nickel Diffusion Coatings, *Anti-Corros. Methods Mater.*, 2003, **50**(2), p 115–120
5. G.R. Kamat, Solid-State Diffusion Welding of Nickel to Stainless Steel, *Weld. J.*, 1988, **67**, p 44–46
6. K.P. Gupta, *Phase Diagram of Ternary Nickel Alloys, Part 1*, Indian Institute of Metals, Calcutta, 1990, p 3
7. T.B. Massalski, *Binary Alloy Phase Diagrams*, 2nd ed., Vol 2, ASM International, Materials Park, OH, 1996, p 1735
8. S. Kundu and S. Chatterjee, Diffusion Bonding Between Commercially Pure Titanium and Micro-Duplex Stainless Steel, *Mater. Sci. Eng. A*, 2008, **480**, p 316–322
9. S. Hinotani and Y. Ohmori, The Use of Kirkendall Effect for Calculating Intrinsic Diffusion Coefficients in a 316L/Ti6242 Diffusion Bonded Couple, *Trans. Jpn. Inst. Met.*, 1988, **29**(2), p 116–124
10. S. Chen, F. Ke, M. Zhou, and Y. Bai, Atomistic Investigation of the Effects of Temperature and Surface Roughness on Diffusion Bonding Between Cu and Al, *Acta Mater.*, 2007, **55**, p 3169–3175
11. B. Derby and E.R. Wallach, Theoretical Model for Diffusion Bonding, *Metal Sci.*, 1982, **16**, p 49–56
12. D.M. Elzey and H.N.G. Wadley, Modeling the Densification of Metal Matrix Composite Monotape, *Acta Metall. Mater.*, 1993, **41**(8), p 2297–2303
13. B. Derby and E.R. Wallach, Diffusion Bonding: Development of Theoretical Model, *Metal Sci.*, 1984, **18**, p 427–432
14. N. Orhan, M. Aksoy, and M. Eroglu, A New Model for Diffusion Bonding and Its Application to Duplex Alloys, *Mater. Sci. Eng. A*, 1999, **271**, p 458–468
15. M.L. Yunker and J.A. Van Orman, Interdiffusion of Solid Iron and Nickel at High Pressure, *Earth Planet. Sci. Lett.*, 2007, **254**, p 203–213
16. G.B. Kale, K. Bhanumurthy, S.K. Khera, and M.K. Asundi, Characteristics of Interdiffusion between 17-4 PH Steel and Nickel, *Mater. Trans.*, 2008, **39**(4), p 733–741
17. M.A. Dayananda and Y.H. Sohn, A New Analysis for the Determination of Ternary Interdiffusion Coefficients from a Single Diffusion Couple, *Mater. Trans. A*, 1999, **30A**, p 535–543
18. A. Laik, P.S. Gawde, K. Bhanumurity, and G.B. Kale, Characteristics of Interdiffusion between 17-4 PH Steel and Nickel, *Metall. Mater. Trans. A*, 2008, **39A**, p 733–741